Front. Energy 2021, 15(3): 568–576
https://doi.org/10.1007/s11708-021-0774-8

MINI REVIEW

Yuichi YAMAGUCHI, Akihiko KUDO

Visible light responsive photocatalysts developed by substitution with metal cations aiming at artificial photosynthesis

Abstract To solve resource, energy, and environmental issues, development of sustainable clean energy system is strongly required. In recent years, hydrogen has been paid much attention to as a clean energy. Solar hydrogen production by water splitting using a photocatalyst as artificial photosynthesis is a promising method to solve these issues. Efficient utilization of visible light comprised of solar light is essential for practical use. Three strategies, i.e., doping, control of valence band, and formation of solid solution are often utilized as the useful methods to develop visible light responsive photocatalysts. This mini-review introduces the recent work on visible-light-driven photocatalysts developed by substitution with metal cations of those strategies.

Keywords visible light responsive photocatalyst, water splitting, artificial photosynthesis: metal ion substitution

1 Introduction

From the viewpoint of the recent resource, energy and environmental issues, development of the sustainable technology is strongly required. Solar water splitting using a photocatalyst is the candidate to solve these issues. When a semiconductor photocatalyst is irradiated with light at an energy more than a band gap, electrons are excited from a valence band to a conduction band of a host material as shown in Fig. 1. Photocatalytic water splitting proceeds when the levels of the conduction band and the valence band are more negative and positive than the redox potentials of H^+/H_2 and O_2/H_2O, respectively. For practical application of solar hydrogen production using a photocatalyst, it is strongly required to develop visible light responsive photocatalysts which split water efficiently under solar light irradiation. The three strategies (doping, control of valence band, and formation of solid solution) described in Fig. 2 are mainly utilized as the useful methods for the development of visible light responsive photocatalyst [1,2].

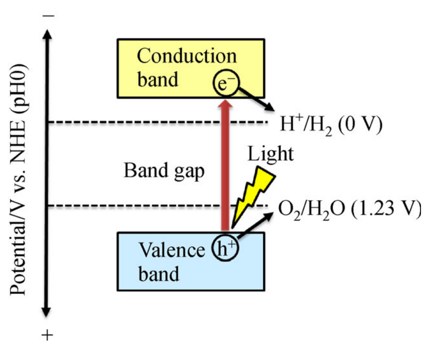

Fig. 1 Illustration of water splitting using a semiconductor photocatalyst.

Doping has often been employed to prepare visible light responsive photocatalysts. Doping means the substitution of a foreign element at the lattice point of host materials, which forms the impurity level in a forbidden band of a semiconductor, bringing response to visible light. Although a dopant contributes to sensitization of a photocatalyst to visible light, it also works as a recombination center which causes the decrease of the photocatalytic activity. Therefore, the optimization of a doping amount is greatly important.

Received Apr. 20, 2021; accepted Jul. 19, 2021; online Sept. 10, 2021

Yuichi YAMAGUCHI, Akihiko KUDO (✉)
Department of Applied Chemistry, Faculty of Science, Tokyo University of Science, Tokyo 162-8601, Japan
E-mail: a-kudo@rs.tus.ac.jp

Special Issue—Photocatalysis: From Solar Light to Hydrogen Energy (Guest Editors: Wenfeng SHANGGUAN, Akihiko KUDO, Zhi JIANG, Yuichi YAMAGUCHI)

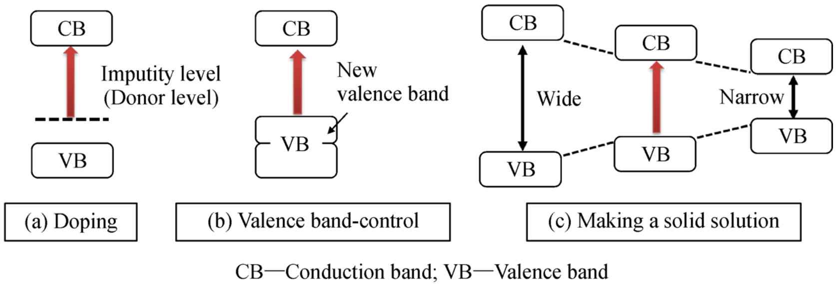

Fig. 2 Strategies for development of a visible light responsive photocatalyst.

In the case of metal oxide semiconductor photocatalysts, the valence band is usually formed by O 2p orbitals and locates at a largely more positive level than an oxidation potential of water. Therefore, the band gap of metal oxide widens to satisfy the sufficient reduction potential of water. Formation of a new valence band is an effective way to solve the issue. $Bi6s^2$ [3], $Pb6s^2$ [4], $Sn5s^2$ [5], $Ag4d^{10}$ [6], and $Cu3d^{10}$ electron-filled orbitals [7] of metal cations form such new valence bands at a more negative level than that of O 2p orbitals, resulting in the development of the photocatalysts having narrow band gaps. Additionally, because N 2p, S 3p, and Se 4p orbitals of non-metal anions composing (oxy) nitride, (oxy) sulfide, and selenide also form valence bands at a more negative level than O 2p orbitals, TaON, Ta_3N_5, graphitic carbon nitride (g-C_3N_4), $Sm_2Ti_2O_5S_2$, $Y_2Ti_2O_5S_2$, and $CuGaSe_2$ are the photocatalysts responding to visible light [8–15]. However, the non-atmospheric condition in the preparation of many valence band-controlled materials is required because they are easily oxidized in air.

Formation of solid solution by combination of several semiconductors having different band gaps is also employed to develop visible light responsive photocatalysts. This strategy is often applied to a chalcogenide photocatalyst. It has a great advantage because the band structure and band gap can easily be tuned by changing the ratio of solid solution [16]. Selection of the materials with a similar crystal structure is required to prepare solid solution photocatalysts.

To use dyes is also one of the methods to sensitize a photocatalyst to visible light [17]. When a dye is irradiated with visible light, an electron is excited from the highest occupied molecular orbital (HOMO) to the lowest unoccupied molecular orbital (LUMO) of the dye and the excited electron transfers to a conduction band of the wide band gap photocatalyst, resulting in the fact that H_2 evolves on the photocatalyst [18,19].

This mini-review introduces doped-, valence band-controlled, and solid solution photocatalysts responding to visible light, developed with metal ion substitution. Inorganic semiconductor photocatalyst materials are especially focused on for water splitting and sacrificial hydrogen and oxygen evolutions aimed at artificial photosynthesis.

2 Doped photocatalysts

Various visible light responsive metal oxide photocatalysts have been developed by doping with transition metal ions such as Ni [20], Cr [21], Rh [22,23], and so on. Rh, Ir, and Ru-doped $SrTiO_3$ photocatalysts are focused on in the present mini-review, because they possess unique properties.

2.1 Rh-doped photocatalyst

A Rh-doped $SrTiO_3$ photocatalyst ($SrTiO_3$:Rh) with 2.3 eV of an energy gap shows a high activity for photocatalytic hydrogen evolution from an aqueous solution containing a sacrificial reagent under visible light irradiation. The Rh^{4+} ions doped in $SrTiO_3$ changes to Rh^{3+} during the photocatalytic reaction. The sacrificial hydrogen evolution proceeds by transition from the impurity levels formed by Rh^{3+} to the conduction band of $SrTiO_3$. In contrast, the $SrTiO_3$:Rh photocatalyst does not show the activity for sacrificial oxygen evolution. Therefore, the $SrTiO_3$:Rh photocatalyst does not singly show the activity for water splitting under visible light irradiation. It can be applied to a Z-schematic water splitting system as a hydrogen-evolving photocatalyst [2,24–26].

The $SrTiO_3$:Rh possesses a unique property as a p-type oxide semiconductor giving cathodic photocurrent under visible light irradiation [27]. Photoelectrochemical water splitting proceeds under visible light irradiation without electrical external bias when the $SrTiO_3$:Rh photocathode is combined with a $BiVO_4$ photoanodes as demonstrated in Fig. 3 [28].

The antipathogens performance using a photocatalyst is also well studied. A TiO_2 photocatalyst, which is a representative photocatalyst, easily inactivates bacteria than bacteriophage under UV light irradiation. In contrast to TiO_2, the $SrTiO_3$:Rh photocatalyst milled by a ball-milling device easily inactivates bacteriophage even in the presence of bacteria under visible light irradiation [29]. The high antiphage performance of the milled $SrTiO_3$:Rh photocatalyst is due to the presence of Rh^{4+} ions induced by visible light irradiation and the large surface area by ball-milling treatment. It is notable that the $SrTiO_3$:Rh

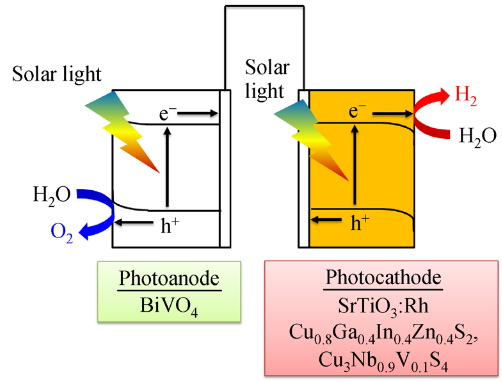

Fig. 3 Photoelectrochemical solar water splitting system consisting of $SrTiO_3$:Rh, $Cu_{0.8}Ga_{0.4}In_{0.4}Zn_{0.4}S_2$, and $Cu_3Nb_{0.9}V_{0.1}S_4$ photocathodes and a $BiVO_4$-based photoanode without any external bias.

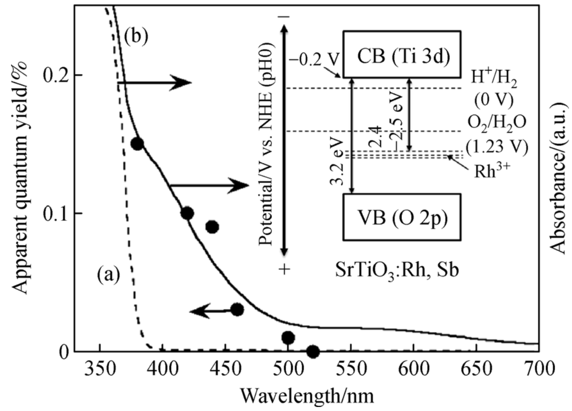

Fig. 4 Diffuse reflectance spectra of non-doped $SrTiO_3$ and $SrTiO_3$:Rh.

(a) Non-doped $SrTiO_3$; (b) $SrTiO_3$:Rh (x(Rh) = 0.5%, x is mole fraction)), Sb (x(Sb) = 1.0%, x is mole fraction)), and an action spectrum for water splitting over IrO_x ($w(IrO_x)$ = 3.0%, w is mass fraction))/$SrTiO_3$:Rh (x(Rh) = 0.5%, x is mole fraction)), Sb ((x(Sb) = 1.0%, x is mole fraction)) photocatalyst (The IrO_x cocatalyst was loaded by an impregnation method at 673 K for 2 h. Photocatalyst: 0.1 g, reactant solution: aqueous H_2SO_4 solution (pH 3.0, 120 mL), light source: 300 W Xe-arc lamp with band-pass filters).

photocatalyst also has a unique property, showing a selective antiphage performance.

In contrast to the single Rh-doped $SrTiO_3$, a Rh and Sb-codoped $SrTiO_3$ photocatalyst ($SrTiO_3$:Rh,Sb) shows photocatalytic activities for both sacrificial hydrogen and oxygen evolutions under visible light irradiation [30] and can split water under visible light irradiation in the presence of an IrO_x cocatalyst [31]. The change in the oxidation number of the Rh ion caused by codoping of Sb plays an important role. Both Rh^{3+} and Rh^{4+} ions exist in $SrTiO_3$:Rh as prepared. On the other hand, when the Rh and Sb ions are codoped in $SrTiO_3$, the Sb ion is doped as Sb^{5+} at a Ti^{4+} site in a $SrTiO_3$ host. Therefore, the oxidation number of Rh^{4+} is controlled to Rh^{3+} due to the charge compensation. Additionally, it is confirmed that the IrO_x cocatalyst enhances the activities for sacrificial hydrogen and oxygen evolutions of $SrTiO_3$:Rh,Sb, which indicates that it works as active sites for both hydrogen and oxygen evolutions on water splitting over an $IrO_x/SrTiO_3$:Rh,Sb photocatalyst. The Rh^{3+} ion and an IrO_x cocatalyst are the key factors for photocatalytic water splitting of $SrTiO_3$:Rh, Sb. $IrO_x/SrTiO_3$:Rh,Sb photocatalyst splits water into H_2 and O_2 stoichiometrically under visible light irradiation of up to 500 nm as depicted in Fig. 4 and shows the activity for solar water splitting [31]. Al-doped $SrTiO_3$, $AgTaO_3$, and $Na_{0.5}Bi_{0.5}TiO_3$ photocatalysts show the high activity for solar water splitting [32–35]. However, those photocatalysts do not respond to visible light. Therefore, it is notable that the $IrO_x/SrTiO_3$:Rh,Sb photocatalyst is the visible light responsive oxide photocatalyst, showing the activity for solar water splitting.

2.2 Ir-doped photocatalyst

$SrTiO_3$:Rh and $SrTiO_3$:Rh,Sb photocatalysts respond to a visible light of up to 540 and 500 nm, respectively. However, it is required to develop the photocatalyst being responsive to longer light wavelength for efficient uses of sunlight. An Ir ion is an effective dopant for response to long wavelength of visible light because the Ir^{3+} ion forms a shallower impurity level in a band gap than the Rh^{3+} ion. Recently, Ir-doped $SrTiO_3$ photocatalyst loaded with Ir cocatalyst ($Ir/SrTiO_3$:Ir) has been developed. The $Ir/SrTiO_3$:Ir photocatalyst treated with H_2 reduction at 673 K shows the activity for sacrificial hydrogen evolution under a visible light of up to approximately 800 nm as exhibited in Fig. 5 [36], indicating that $Ir/SrTiO_3$:Ir can utilize the whole range of visible light. The Ir ion is mainly doped as Ir^{4+} at a Ti^{4+} site in a $SrTiO_3$ host as prepared. After H_2 reduction and sacrificial hydrogen evolution, it was confirmed by diffuse reflectance spectra that the oxidation number of the Ir^{4+} ion changed to Ir^{3+}. The sacrificial hydrogen evolution proceeds by transition from the impurity levels formed by Ir^{3+} to the conduction band of $SrTiO_3$. In addition, an Ir cocatalyst plays an important role in the activity for hydrogen evolution over $Ir/SrTiO_3$Ir. H_2 reduction contributes to the formation of metallic Ir and a good contact between the loaded Ir and $SrTiO_3$:Ir host. By these synergistic effects, an Ir cocatalyst works as an efficient site for hydrogen evolution.

$NaNbO_3$ and $BaTa_2O_6$ codoped with Ir ions and alkali earth metal ions or lanthanum ions have also been reported as visible light responsive photocatalysts [37,38]. The Ir ion is doped as Ir^{3+} by codoping with Ca^{2+}, Sr^{2+}, Ba^{2+}, and La^{3+} due to charge compensation. $NaNbO_3$ codoped with Ir and Sr ions shows the activity for both sacrificial hydrogen and oxygen evolutions under visible light irradiation and responds to a visible light of up to

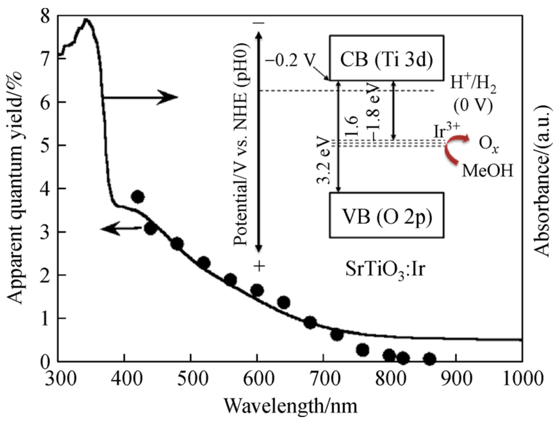

Fig. 5 A diffuse reflectance spectrum and an action spectrum for sacrificial hydrogen evolution over Ir ($w(IrO_x)$ = 0.86%, w is mass fraction))/$SrTiO_3$:Ir (x(Ir) = 0.2%, x is mole fraction)) photocatalyst (The Ir cocatalyst was loaded by an impregnation method at 673 K for 2 h and subsequent H_2-reduction at 673 K for 1 h. Photocatalyst: 0.2 g, reactant solution: aqueous methanol solution (φ(methanol) = 10%, φ is volume fraction, 120 mL), light source: 300 W Xe-arc lamp with band-pass filters).

700 nm for sacrificial hydrogen evolution. In addition, $NaTaO_3$ and $BaTa_2O_6$ codoped with Ir and La ions shows the photocatalytic activity for sacrificial hydrogen evolution under a visible light of up to 600 and 640 nm, respectively. It suggests that the Ir ion is a suitable dopant for sensitization of a metal oxide photocatalyst to a long wavelength of visible light.

2.3 Ru-doped photocatalyst

Previously, a Ru-doped $SrTiO_3$ ($SrTiO_3$:Ru) photocatalyst showing the activity for both hydrogen and oxygen evolutions from aqueous solutions containing sacrificial reagents under visible light irradiation is reported [22]. This photocatalyst is a unique material which is active for both sacrificial hydrogen and oxygen evolutions by doping of a single metal ion. However, the photocatalytic properties have not been clarified so far. Thus, effects of co-doping and H_2 reduction to $SrTiO_3$:Ru on photocatalytic properties are expected. It is confirmed by electron spin resonance spectra and diffuse reflectance spectra that the oxidation number of a Ru dopant is controlled to trivalent by co-doping of a Sb^{5+} ion and H_2 reduction [39]. While the activities for sacrificial hydrogen evolution over $SrTiO_3$:Ru, Sb and H_2-red. $SrTiO_3$:Ru are lower than that over pristine $SrTiO_3$:Ru, the activities for sacrificial oxygen evolution are higher than that over pristine $SrTiO_3$:Ru. In particular, the activity over $SrTiO_3$:Ru treated with H_2 at 673 K is the highest among those photocatalysts, which shows a higher activity of about four times than pristine $SrTiO_3$:Ru. It is notable that H_2-red. $SrTiO_3$:Ru shows the activity for sacrificial oxygen evolution under a visible light of up to 750 nm.

3 Valence band-controlled photocatalysts developed by metal ion exchange for alkali ions in various metal oxides using molten salts treatment

$BiVO_4$ and $SnNb_2O_6$ are the representative valence band-controlled photocatalysts [3,5,40–42]. On the other hand, the novel visible light responsive photocatalyst can be developed by metal ion exchange of the alkali ion in metal oxides. The Ag(I) and Cu(I) ions contribute to forming a shallow valence band in oxide materials [6,43,44]. However, it is difficult to prepare the materials containing Ag(I) and Cu(I) ions by conventional solid state reaction because of the formation of Ag(0) and Cu(II). In such a background, the visible light responsive photocatalysts containing the Ag(I) and Cu(I) ions have been successfully developed by treatments of layered oxide materials with molten $AgNO_3$ and CuCl. Herein, various visible light responsive photocatalysts developed by Ag(I) and Cu(I) ions exchange of the alkali ions in various metal oxides by molten salts treatment are described.

3.1 Ag(I) ion-exchanged metal oxide photocatalysts with a layered structure

Photocatalytic activity for sacrificial oxygen evolution over various Ag(I) ion-exchanged layered oxide materials is listed in Table 1.

$Na_2W_4O_{13}$ consists of layered structure of $[W_4O_{13}]^{2-}$ slabs and Na^+ ions in the interlayer as displayed in Fig. 6. $Na_2W_4O_{13}$ cannot absorb visible light because its band gap

Table 1 Ag(I) ion-exchanged layered oxide photocatalysts showing a sacrificial oxygen evolution activity under visible light irradiation

Photocatalyst	Crystal structure	BG(EG)/eV	O_2 evolution/(μmol·h^{-1})
Ag(I)-$Na_2W_4O_{13}$	Layered	2.8	4
Ag(I)-$K_2SrTa_2O_7$	RP[a]	2.8	3
Ag(I)-$K_2SrNb_{0.2}Ta_{1.8}O_7$	RP[a]	2.8	4
Ag(I)-$K_2CaNaNb_3O_{10}$	RP[a]	3.0	2
Ag(I)-$KLaNb_2O_7$	DJ[b]	2.9–3.1	2
Ag(I)-$Li_2SrTa_2O_7$	DJ[b]	2.8	4

Notes: Photocatalyst: 0.1–0.5 g; reactant solution: 20 mmol/L $AgNO_3$ (aq.) (120 mL); light source: 300 W Xe-arc lamp with a cutoff filter (HOYA: L42) ($\lambda > 420$ nm); [a]—Ruddlesden-Popper-type layered perovskite structure; [b]—Dion-Jacobson-type layered perovskite structure.

is 3.12 eV. When $Na_2W_4O_{13}$ is treated with molten $AgNO_3$, Na^+ ions are exchanged with Ag^+ ions, keeping the layered structure, which results in the formation of a new valence band consisting of Ag4d orbitals, leading to the photocatalytic activity for the sacrificial oxygen evolution under visible light irradiation [45]. The Ag(I) ion-exchanged $Na_2W_4O_{13}$ photocatalyst responds to a visible light of up to 440 nm at which non-ion-exchanged $Na_2W_4O_{13}$ cannot show the activity. Additionally, Z-schematic water splitting using the Ag(I) ion-exchanged $Na_2W_4O_{13}$ as an oxygen-evolving photocatalyst with a $SrTiO_3$:Rh photocatalyst of a hydrogen-evolving photocatalyst proceeds under visible light irradiation.

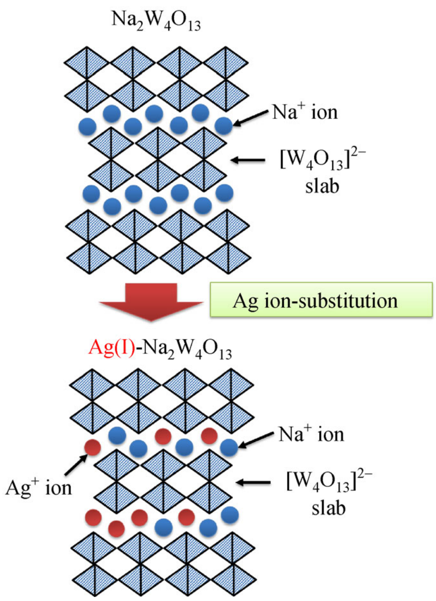

Fig. 6 Illustration of preparation of Ag(I)-substituted $Na_2W_4O_{13}$ by molten $AgNO_3$ treatment.

Many metal oxide photocatalysts with Ruddlesden-Popper-type and Dion-Jacobson-type layered perovskite structures synthesized by molten $AgNO_3$ treatment such as Ag(I)-$A_2SrTa_2O_7$ (A = Li, K), Ag(I)-$K_2SrNb_{0.2}Ta_{1.8}O_7$, Ag(I)-$K_2CaNaNb_3O_{10}$, and Ag(I)-$KLaNb_2O_7$ are active for sacrificial oxygen evolution under light irradiation [46]. The visible light response is attributed to photoexcitation of electrons from a valence band consisting of Ag4d and O2p orbitals to a conduction band of layered oxides of host materials. In general, Ag(I) ions in interlayer to metallic Ag are usually reduced by photoexcited electrons, leading to the deactivation of the photocatalyst. However, the XRD pattern of Ag(I)-$K_2SrTa_2O_7$ of a representative Ag(I) ion-exchanged material hardly changes even after the photocatalytic sacrificial oxygen evolution for 5 h. This indicates that the Ag(I) ions in the interlayers of Ag(I)-$K_2SrTa_2O_7$ are relatively stable against the reduction.

3.2 Cu(I) ion-exchanged metal oxide photocatalysts with a layered and tunneling structure

Photocatalytic activity for sacrificial hydrogen evolution over various Cu(I) ion-exchanged layered materials is summarized in Table 2.

Cu(I) ion-exchanged Li_2TiO_3 ($CuLi_{1/3}Ti_{2/3}O_2$) with a delafossite structure has trigonal and hexagonal phases. Although it was reported that the hexagonal $CuLi_{1/3}Ti_{2/3}O_2$ photocatalyst showing the sacrificial hydrogen evolution under visible light irradiation was successfully prepared by a flux method [47], the single phase of trigonal had not been prepared so far. Cubic Li_2TiO_3 of a low temperature phase and monoclinic Li_2TiO_3 of a high temperature phase have a bulky structure and layered crystal structures, respectively. Hexagonal $CuLi_{1/3}Ti_{2/3}O_2$ and trigonal $CuLi_{1/3}Ti_{2/3}O_2$ can be selectively prepared in a single phase by a molten CuCl treatment of cubic and monoclinic Li_2TiO_3 [48]. The band gaps of hexagonal and trigonal $CuLi_{1/3}Ti_{2/3}O_2$ are 2.1 eV and they show the activity for

Table 2 Cu(I) ion-exchanged oxide photocatalysts showing a sacrificial hydrogen evolution activity under visible light irradiation

Photocatalyst	Crystal structure	BG(EG)/eV	Incident light/nm	H_2 evolution/(μmol·h^{-1})
$CuLi_{1/3}Ti_{2/3}O_2$ (hex.)	Delafossite (-like)	2.1	> 440	130
$CuLi_{1/3}Ti_{2/3}O_2$ (tri.)	Delafossite (-like)	2.1	> 440	105
Cu(I)-$K_2SrTa_2O_7$	RP[a]	2.1	> 420	66
Cu(I)-$Na_2La_2Ti_3O_{10}$	RP[a]	2.0	> 420	0.8
Cu(I)-$K_2La_2Ti_3O_{10}$	RP[a]	2.0	> 420	45
Cu(I)-$KLaTa_2O_7$	DJ[b]	2.9	> 420	0.2
Cu(I)-$Li_2Na_2Ti_6O_{14}$	TN[c]	2.6	> 440	0.9
Cu(I)-$Li_2SrTi_6O_{14}$	TN[c]	2.1	> 440	2
Cu(I)-$Li_2BaTi_6O_{14}$	TN[c]	2.1	> 440	0.7
Cu(I)-$Li_2PbTi_6O_{14}$	TN[c]	2.1	> 440	0.8

Notes: Photocatalyst: 0.1–0.5 g; cocatalyst: Ru (w(Ru) = 0.3%, w is mass fraction); reactant solution: 0.5 mol/L K_2SO_3 + 0.1 mol/L Na_2S (aq.) (120 mL); light source: 300 W Xe-arc lamp with cutoff filters (HOYA: L42, Y44); [a]—Ruddlesden-Popper-type layered perovskite structure; [b]—Dion-Jacobson-type layered perovskite structure; [c]—Tunneling structure.

photocatalytic hydrogen evolution from an aqueous solution containing sacrificial reagent under a visible light of up to about 600 nm. In addition, Z-schematic water splitting proceeds under solar light irradiation using those Pt-loaded $CuLi_{1/3}Ti_{2/3}O_2$ as hydrogen-evolving photocatalysts, a TiO_2 as an oxygen-evolving photocatalyst, and a reduced graphene oxide (RGO) as a solid-state electron mediator as shown in Fig. 7.

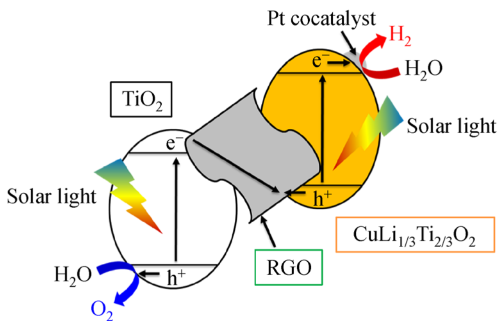

Fig. 7 Z-schematic solar water splitting system consisting of a Pt-loaded $CuLi_{1/3}Ti_{2/3}O_2$ as a hydrogen-evolving photocatalyst, a TiO_2 as an oxygen-evolving photocatalyst, and an RGO as a solid-state electron mediator.

Various Cu(I) ion-exchanged Ruddlesden-Popper(RP)-type and Dion-Jacobson(DJ)-type layered perovskite metal oxides have also been developed [46,49], among which, RP-type metal oxides consisting of Ti(IV) or Ta(V) in the perovskite slabs, and K(I) in the interlayer are suitable host materials to obtain visible light responsive photocatalysts by Cu(I) ion exchange. In particular, Cu(I)-$K_2SrTa_2O_7$ photocatalyst with an RP structure shows the highest activity for sacrificial hydrogen evolution under a visible light irradiation of up to 600 nm. Although Cu(I)-$KLaTa_2O_7$ with a DJ structure has a similar slab to Cu (I)-$K_2SrTa_2O_7$, the photocatalytic activity of the Cu(I)-$KLaTa_2O_7$ is much lower than that of Cu(I)-$K_2SrTa_2O_7$. The difference in the photocatalytic activity is due to the density of the Cu(I) ion and the interaction between the Cu(I) ion at the interlayer in the photocatalyst. The high density of the Cu(I) ions is favorable for the migration of photogenerated holes to the edges of layered structure of photocatalyst particles because Cu(I) forms the valence band. On the other hand, even if Cu(I) ion-exchanged $M_2La_2Ti_3O_{10}$ (M = K, Na) photocatalysts possess the same layered structure as each other, Cu(I)-$K_2La_2Ti_3O_{10}$ shows a much higher activity than Cu(I)-$Na_2La_2Ti_3O_{10}$. It is confirmed that Cu(I)-$Na_2La_2Ti_3O_{10}$ contains Cu(II) impurities that work as a recombination center between photogenerated e^- and h^+. These studies reveal that not only the intrinsic property of the host material and the rate of ion exchange but also the density of the Cu(I) ions exchanged in the interlayers and the formation of unfavorable Cu(II) species affect the photocatalytic activity.

Cu(I)-$Li_2MTi_6O_{14}$ (M = Na_2, Sr, Ba, Pb) with a tunneling structure is also successfully developed by Cu(I) ion exchange for the alkali ions in the tunnel [46], of which, Cu(I)-$Li_2SrTi_6O_{14}$ shows the highest activity for sacrificial hydrogen evolution responding to a visible light of up to 560 nm. This study is of great significance in terms of the successful development of visible-light-driven photocatalyst from a wide-band-gap photocatalyst with a tunneling structure by Cu(I) ion exchange.

4 Solid solution photocatalysts

Solid solution has often been applied to develop visible light responsive photocatalysts based on a calcogenide-type photocatalyst. Although photocorrosion of a metal sulfide photocatalyst easily occurs in general, it is suppressed by using a suitable reducing reagent of sacrificial electron donor such as S^{2-} or SO_3^{2-}. Many metal sulfide photocatalysts containing the Cu(I) ion show a p-type semiconductor character and can be employed as a photocathode in a photoelectrochemical water splitting system. Construction of the system responsive to visible light by employing a sulfide photocatalyst as a photocathode and an n-type semiconductor photocatalyst as a photoanode is a significant research topic.

$CuGaS_2$-$AgGaS_2$ [50], ZnS-$CuGaS_2$ [51], and ZnS-$CuGaS_2$-$CuInS_2$ [52] solid solution photocatalysts have been developed. The optimal ratio of these solid solutions on photocathodic property are $Cu_{0.8}Ag_{0.2}GaS_2$ (BG: 2.2 eV), $(CuGa)_{0.5}ZnS_2$ (BG: 1.9 eV), and $Cu_{0.8}Ga_{0.4}In_{0.4}Zn_{0.4}S_2$ (BG: 2.35 eV), respectively. By employing a $Cu_{0.8}Ga_{0.4}In_{0.4}Zn_{0.4}S_2$-based photocathode and a $BiVO_4$-based photoanode as shown in Fig. 2, solar water splitting proceeds without any external bias.

Cu_3MS_4 (M = V, Nb, Ta) with a sulvanite structure is also the promising photocatalyst which shows the activity for sacrificial hydrogen evolution under visible light irradiation [53,54]. The band gaps of Cu_3VS_4, Cu_3NbS_4, and Cu_3TaS_4 are 1.6, 2.5, and 2.8 eV, respectively. Solid solutions using those photocatalysts, such as $Cu_3Nb_{1-x}V_xS_4$ and $Cu_3Ta_{1-x}V_xS_4$, show higher activities than the single component Cu_3MS_4 (M = V, Nb, Ta). The band gaps of those solid solutions are 1.6–1.7 eV, indicating the absorption of a wide range of visible light. In particular, the $Cu_3Nb_{0.9}V_{0.1}S_4$ solid solution shows the highest photocatalytic activity among those solid solutions. Additionally, the $Cu_3Nb_{1-x}V_xS_4$ and $Cu_3Ta_{1-x}V_xS_4$ give cathodic photocurrents under visible light irradiation, indicating that those solid solutions show a p-type semiconductor character, among which, the $Cu_3Nb_{0.9}V_{0.1}S_4$ shows the best photoelectrochemical performance. When the system consisting of Ru-loaded $Cu_3Nb_{0.9}V_{0.1}S_4$ as a photocathode and $BiVO_4$ loaded with CoO_x cocatalyst as a photoanode is constructed as shown in Fig. 3, the photoelectrochemical water splitting proceeds under simulated sunlight irradiation. This result indicates that the formation of solid solutions is effective for Cu_3MS_4 (M = V, Nb, Ta)-based photocatalysts and photoelectrodes.

5 Conclusions

Various visible light responsive photocatalysts were developed by metal ion exchange. For doped-photocatalysts, a $SrTiO_3$:Rh showed a high activity for sacrificial hydrogen evolution under visible light irradiation and functioned as a photocathode in a photoelectrochemical system. $IrO_x/SrTiO_3$:Rh,Sb of a single particulate photocatalyst was also a promising photocatalyst which showed the activity for water splitting under visible light irradiation. Moreover, Ir and Ru were also an excellent dopant for sensitization of a photocatalyst to long wavelength of visible light. In particular, a Ir/$SrTiO_3$:Ir treated with H_2 showed the activity for sacrificial hydrogen evolution responding up to the whole range of a visible light of up to 800 nm. For valence band-controlled photocatalysts, various visible light responsive metal oxides with layered and tunneling structures were developed by exchange of the alkali ions in the metal oxides with Ag(I) and Cu(I) ions by molten salts treatment, among which, a $CuLi_{1/3}Ti_{1/3}O_2$ photocatalyst with a delafossite-like structure and a Cu(I)-$K_2SrTa_2O_7$ photocatalyst with a Ruddlesden-Popper-type layered structure showed a relatively high activity for sacrificial hydrogen evolution under visible light irradiation. For solid solution photocatalysts, $CuGaS_2$-$AgGaS_2$, ZnS-$CuGaS_2$, ZnS-$CuGaS_2$-$CuInS_2$, and Cu_3MS_4(M = V, Nb, Ta) photocatalysts which showed the activity for sacrificial hydrogen evolution under visible light were developed. In particular, $Cu_3Nb_{0.9}V_{0.1}S_4$ photocatalyst and photocathode showed a higher activity for sacrificial hydrogen evolution and a larger photocurrent than the single component Cu_3VS_4 and Cu_3NbS_4. This indicates that the formation of a solid solution is also an effective way to improve photocatalytic and photoelectrochemical performances.

For practical use of photocatalytic water splitting for hydrogen production, it is strongly required to develop the photocatalyst responding to the long wavelength of visible light and having a high quantum yield. Although the number of reported photocatalysts responding to a long wavelength of light is increasing, that of photocatalysts with a high quantum yield is still limited. The development of highly activated photocatalysts responsive to long wavelength visible lights can be achieved by further improving the preparation method. If the strategy of the design of a photocatalyst with a high quantum efficiency is clarified, great progresses will be made in this research area. It is expected that the photocatalytic water splitting technology is applicable for practical use by development of novel visible-light-driven photocatalysts.

Acknowledgements This work was supported by JSPS KAKENHI (Grant Nos. 17H06433 and 17H06440) in Scientific Research on Innovative Areas "Innovations for Light-Energy Conversion (I4 LEC)," 17H01217, and 20K15383.

References

1. Kudo A, Kato H, Tsuji I. Strategies for the development of visible-light-driven photocatalysts for water splitting. ChemInform, 2004, 33(12): 1534–1539
2. Kudo A, Miseki Y. Heterogeneous photocatalyst materials for water splitting. Chemical Society Reviews, 2009, 38(1): 253–278
3. Kudo A, Omori K, Kato H. A novel aqueous process for preparation of crystal form-controlled and highly crystalline $BiVO_4$ powder from layered vanadates at room temperature and its photocatalytic and photophysical properties. Journal of the American Chemical Society, 1999, 121(49): 11459–11467
4. Shimodaira Y, Kato H, Kobayashi H, et al. Investigations of electronic structures and photocatalytic activities under visible light irradiation of lead molybdate replaced with chromium(VI). Bulletin of the Chemical Society of Japan, 2007, 80(5): 885–893
5. Hosogi Y, Shimodaira Y, Kato H, et al. Role of Sn^{2+} in the band structure of SnM_2O_6 and $Sn_2M_2O_7$ (M = Nb and Ta) and their photocatalytic properties. Chemistry of Materials, 2008, 20(4): 1299–1307
6. Kato H, Kobayashi H, Kudo A. Role of Ag^+ in the band structures and photocatalytic properties of $AgMO_3$ (M: Ta and Nb) with the perovskite structure. Journal of Physical Chemistry B, 2002, 106(48): 12441–12447
7. Joshi U A, Palasyuk A M, Maggard P A. Photoelectrochemical investigation and electronic structure of a *p*-type $CuNbO_3$ photocathode. Journal of Physical Chemistry C, 2011, 115(27): 13534–13539
8. Maeda K, Domen K. New non-oxide photocatalysts designed for overall water splitting under visible light. Journal of Physical Chemistry C, 2007, 111(22): 7851–7861
9. Hitoki G, Takata T, Kondo J N, et al. An oxynitride, TaON, as an efficient water oxidation photocatalyst under visible light irradiation ($\lambda \leqslant 500$ nm). Chemical Communications (Cambridge), 2002, (16): 1698–1699
10. Hara M, Hitoki G, Takata T, et al. TaON and Ta_3N_5 as new visible light driven photocatalysts. Catalysis Today, 2003, 78(1–4): 555–560
11. Wang X, Maeda K, Thomas A, et al. A metal-free polymeric photocatalyst for hydrogen production from water under visible light. Nature Materials, 2009, 8(1): 76–80
12. Wen J, Xie J, Chen X, et al. A review on g-C_3N_4-based photocatalysts. Applied Surface Science, 2017, 391: 72–123
13. Ishikawa A, Takata T, Kondo J N, et al. Oxysulfide $Sm_2Ti_2S_2O_5$ as a stable photocatalyst for water oxidation and reduction under visible light irradiation ($\lambda \leqslant 650$ nm). Journal of the American Chemical Society, 2002, 124(45): 13547–13553
14. Wang Q, Nakabayashi M, Hisatomi T, et al. Oxysulfide photocatalyst for visible-light-driven overall water splitting. Nature Materials, 2019, 18(8): 827–832

15. Moriya M, Minegishi T, Kumagai H, et al. Stable hydrogen evolution from CdS-modified $CuGaSe_2$ photoelectrode under visible-light irradiation. Journal of the American Chemical Society, 2013, 135(10): 3733–3735
16. Tsuji I, Kato H, Kudo A. Visible-light-induced H_2 evolution from an aqueous solution containing sulfide and sulfite over a ZnS-$CuInS_2$-$AgInS_2$ solid-solution photocatalyst. Angewandte Chemie International Edition, 2005, 44(23): 3565–3568
17. Kajiwara T, Hashimoto K, Kawai T, et al. Dynamics of luminescence from $Ru(bpy)_3Cl_2$ adsorbed on semiconductor surfaces. Journal of Physical Chemistry, 1982, 86(23): 4516–4522
18. Abe R, Hara K, Sayama K, et al. Steady hydrogen evolution from water on Eosin Y-fixed TiO_2 photocatalyst using a silane-coupling reagent under visible light irradiation. Journal of Photochemistry and Photobiology A Chemistry, 2000, 137(1): 63–69
19. Maeda K, Eguchi M, Lee S H A, et al. Photocatalytic hydrogen evolution from hexaniobate nanoscrolls and calcium niobate nanosheets sensitized by ruthenium(II) bipyridyl complexes. Journal of Physical Chemistry C, 2009, 113(18): 7962–7969
20. Niishiro R, Kato H, Kudo A. Nickel and either tantalum or niobium-codoped TiO_2 and $SrTiO_3$ photocatalysts with visible-light response for H_2 or O_2 evolution from aqueous solutions. Physical Chemistry Chemical Physics, 2005, 7(10): 2241–2245
21. Kato H, Kudo A. Visible-light-response and photocatalytic activities of TiO_2 and $SrTiO_3$ photocatalysts codoped with antimony and chromium. Journal of Physical Chemistry B, 2002, 106(19): 5029–5034
22. Konta R, Ishii T, Kato H, et al. Photocatalytic activities of noble metal ion doped $SrTiO_3$ under visible light irradiation. The Journal of Physical Chemistry B, 2004, 108(26): 8992–8995
23. Niishiro R, Konta R, Kato H, et al. Photocatalytic O_2 evolution of rhodium and antimony-codoped rutile-type TiO_2 under visible light irradiation. Journal of Physical Chemistry C, 2007, 111(46): 17420–17426
24. Kato H, Hori M, Konta R, et al. Construction of Z-scheme type heterogeneous photocatalysis systems for water splitting into H_2 and O_2 under visible light irradiation. Chemistry Letters, 2004, 33(10): 1348–1349
25. Sasaki Y, Kato H, Kudo A. $Co(bpy)_3]^{3+/2+}$ and $[co(phen)_3]^{3+/2+}$ electron mediators for overall water splitting under sunlight irradiation using Z-scheme photocatalyst system. Journal of the American Chemical Society, 2013, 135(14): 5441–5449
26. Jia Q, Iwase A, Kudo A. $BiVO_4$–Ru/$SrTiO_3$: Rh composite Z-scheme photocatalyst for solar water splitting. Chemical Science (Cambridge), 2014, 5(4): 1513
27. Iwashina K, Kudo A. Rh-doped $SrTiO_3$ photocatalyst electrode showing cathodic photocurrent for water splitting under visible-light irradiation. Journal of the American Chemical Society, 2011, 133(34): 13272–13275
28. Jia Q, Iwashina K, Kudo A. Facile fabrication of an efficient $BiVO_4$ thin film electrode for water splitting under visible light irradiation. Proceedings of the National Academy of Sciences of the United States of America, 2012, 109(29): 11564–11569
29. Yamaguchi Y, Usuki S, Kanai Y, et al. Selective inactivation of bacteriophage in the presence of bacteria by use of ground Rh-doped $SrTiO_3$ photocatalyst and visible light. ACS Applied Materials & Interfaces, 2017, 9(37): 31393–31400
30. Niishiro R, Tanaka S, Kudo A. Hydrothermal-synthesized $SrTiO_3$ photocatalyst codoped with rhodium and antimony with visible-light response for sacrificial H_2 and O_2 evolution and application to overall water splitting. Applied Catalysis B: Environmental, 2014, 150–151: 187–196
31. Asai R, Nemoto H, Jia Q, et al. A visible light responsive rhodium and antimony-codoped $SrTiO_3$ powdered photocatalyst loaded with an IrO_2 cocatalyst for solar water splitting. Chemical Communications: Cambridge, England, 2014, 50(19): 2543–2546
32. Lyu H, Hisatomi T, Goto Y, et al. An Al-doped $SrTiO_3$ photocatalyst maintaining sunlight-driven overall water splitting activity for over 1000 h of constant illumination. Chemical Science (Cambridge), 2019, 10(11): 3196–3201
33. Takata T, Jiang J, Sakata Y, et al. Photocatalytic water splitting with a quantum efficiency of almost unity. Nature, 2020, 581(7809): 411–414
34. Watanabe K, Iwase A, Kudo A. Solar water splitting over $Rh_{0.5}Cr_{1.5}O_3$-loaded $AgTaO_3$ of a valence-band-controlled metal oxide photocatalyst. Chemical Science (Cambridge), 2020, 11(9): 2330–2334
35. Watanabe K, Iikubo Y, Yamaguchi Y, et al. Highly crystalline $Na_{0.5}Bi_{0.5}TiO_3$ of a photocatalyst valence-band-controlled with Bi (III) for solar water splitting. Chemical Communications, 2021, 57(3): 323–326
36. Suzuki S, Matsumoto H, Iwase A, et al. Enhanced H_2 evolution over an Ir-doped $SrTiO_3$ photocatalyst by loading of an Ir cocatalyst using visible light up to 800 nm. Chemical Communications: Cambridge, England, 2018, 54(75): 10606–10609
37. Iwase A, Saito K, Kudo A. Sensitization of $NaMO_3$ (M: Nb and Ta) photocatalysts with wide band gaps to visible light by Ir doping. Bulletin of the Chemical Society of Japan, 2009, 82(4): 514–518
38. Iwase A, Kudo A. Development of Ir and La-codoped $BaTa_2O_6$ photocatalysts using visible light up to 640 nm as an H_2-evolving photocatalyst for Z-schematic water splitting. Chemical Communications: Cambridge, England, 2017, 53(45): 6156–6159
39. Suzuki S, Iwase A, Kudo A. Long wavelength visible light-responsive $SrTiO_3$ photocatalysts doped with valence-controlled Ru for sacrificial H_2 and O_2 evolution. Catalysis Science & Technology, 2020, 10(15): 4912–4916
40. Kudo A, Ueda K, Kato H, et al. Photocatalytic O_2 evolution under visible light irradiation on $BiVO_4$ in aqueous $AgNO_3$ solution. Catalysis Letters, 1998, 53(3/4): 229–230
41. Tokunaga S, Kato H, Kudo A. Selective preparation of monoclinic and tetragonal $BiVO_4$ with scheelite structure and their photocatalytic properties. Chemistry of Materials, 2001, 13(12): 4624–4628
42. Hosogi Y, Tanabe K, Kato H, et al. Energy structure and photocatalytic activity of niobates and tantalates containing Sn(II) with a $5s^2$ electron configuration. Chemistry Letters, 2004, 33(1): 28–29
43. Konta R, Kato H, Kobayashi H, et al. Photophysical properties and photocatalytic activities under visible light irradiation of silver vanadates. Physical Chemistry Chemical Physics, 2003, 5(14): 3061
44. Boltersdorf J, Maggard P A. Silver exchange of layered metal oxides and their photocatalytic activities. ACS Catalysis, 2013, 3(11):

2547–2555

45. Horie H, Iwase A, Kudo A. Photocatalytic properties of layered metal oxides substituted with silver by a molten $AgNO_3$ treatment. ACS Applied Materials & Interfaces, 2015, 7(27): 14638–14643
46. Watanabe K, Iwashina K, Iwase A, et al. New visible-light-driven H_2^- and O_2^- evolving photocatalysts developed by Ag(I) and Cu(I) ion exchange of various layered and tunneling metal oxides using molten salts treatments. Chemistry of Materials, 2020, 32(24): 10524–10537
47. Kato H, Fujisawa T, Kobayashi M, et al. Discovery of novel delafossite-type compounds composed of copper(I) lithium titanium with photocatalytic activity for H_2 evolution under visible light. Chemistry Letters, 2015, 44(7): 973–975
48. Iwashina K, Iwase A, Nozawa S, et al. Visible-light-responsive $CuLi_{1/3}Ti_{2/3}O_2$ powders prepared by a molten CuCl treatment of Li_2TiO_3 for photocatalytic H_2 evolution and Z-schematic water splitting. Chemistry of Materials, 2016, 28(13): 4677–4685
49. Iwashina K, Iwase A, Kudo A. Sensitization of wide band gap photocatalysts to visible light by molten CuCl treatment. Chemical Science (Cambridge), 2015, 6(1): 687–692
50. Kaga H, Tsutsui Y, Nagane A, et al. An effect of Ag(I)-substitution at Cu sites in $CuGaS_2$ on photocatalytic and photoelectrochemical properties for solar hydrogen evolution. Journal of Materials Chemistry A, Materials for Energy and Sustainability, 2015, 3(43): 21815–21823
51. Kato T, Hakari Y, Ikeda S, et al. Utilization of metal sulfide material of $(CuGa)_{1-x}Zn_{2x}S_2$ solid solution with visible light response in photocatalytic and photoelectrochemical solar water splitting systems. Journal of Physical Chemistry Letters, 2015, 6(6): 1042–1047
52. Hayashi T, Niishiro R, Ishihara H, et al. Powder-based $(CuGa_{1-y}In_y)_{1-x}Zn_{2x}S_2$ solid solution photocathodes with a largely positive onset potential for solar water splitting. Sustainable Energy & Fuels, 2018, 2(9): 2016–2024
53. Ikeda S, Aono N, Iwase A, et al. Cu_3MS_4 (M = V, Nb, Ta) and its solid solutions with sulvanite structure for photocatalytic and photoelectrochemical H_2 evolution under visible-light irradiation. ChemSusChem, 2019, 12(9): 1977–1983
54. Takayama T, Tsuji I, Aono N, et al. Development of various metal sulfide photocatalysts consisting of d^0, d^5, and d^{10} metal ions for sacrificial H_2 evolution under visible light irradiation. Chemistry Letters, 2017, 46(4): 616–619